

Received March 18, 2020, accepted March 26, 2020, date of publication March 30, 2020, date of current version April 16, 2020.

Digital Object Identifier 10.1109/ACCESS.2020.2984153

Single-Layer High Gain Endfire Antenna Based on Spoof Surface Plasmon Polaritons

LEILEI LIU^{1,2}, (Member, IEEE), MINGHONG CHEN¹, AND XIAOXING YIN², (Member, IEEE)

¹National and Local Joint Engineering Laboratory of RF Integration and Micro-Assembly Technology, College of Electronic and Optical Engineering, Nanjing University of Posts and Telecommunications, Nanjing 210003, China

²State Key Laboratory of Millimeter Waves, Southeast University, Nanjing 210096, China

Corresponding author: Leilei Liu (liull@njupt.edu.cn)

This work was supported in part by the Open Research Fund of the National and Local Joint Engineering Laboratory of RF Integration and Micro-Assembly Technology under Grant KFJJ20180101, in part by the State Key Laboratory of Millimeter Waves Open Research Program under Grant K201827, in part by the Natural Science Foundation of China under Grant U1536124, and in part by the Postgraduate Research and Practice Innovation Program of Jiangsu Province under Grant KYCX18_0875.

ABSTRACT A novel high gain endfire antenna based on the spoof surface plasmon polaritons (SSPP) transmission line (TL) is proposed in this paper. The antenna is designed on a groundless single metal layer inherited the advantages of SSPP. Combined with asymmetric radiation elements of SSPP TL and an elliptical director, this antenna generates endfire radiation beams with 15.75–17.5 GHz. Although the aperture is small, it has obtained a high gain from 10.5 to 12.1 dBi and a high efficiency of 95% overall the operating bandwidth. Measurement results agree well with the simulations. The advantages of single-layer, high gain and low profile make its valuable in wireless communications.

INDEX TERMS Endfire, spoof surface plasmon polaritons (SSPP), single-layer.

I. INTRODUCTION

Spoof surface plasmon polaritons (SSPP) have inspired an intensive interest in the microwave community, whose characteristics are similar to surface plasmon polaritons (SPP) in the optical frequencies [1]. With periodic metal structures, such as grooves [2], holes [3], [4], slits [5], or blocks [6], the transversal magnetic surface waves can be sustained and guided. For the groundless structure and small power loss, SSPP have been used to design microwave components, such as transmission line [7], [8], power dividers [9], filters [10], [11], amplifiers [12], and antennas [13]–[24]. Since the phase mismatch with the free space, SSPP wave is highly confined to the transmission line. In order to excite the radiation into the free space, the field confinement of SSPP should be to break.

As SSPP TLs are slow wave structures in which phase velocity is smaller than the speed of light, traveling wave antennas are well suited to its advantages. Several works have been demonstrated such as leaky-wave antennas [13]–[16] and endfire antennas [17]–[24]. There are several types of endfire antenna, such as leaky-wave [25], Yagi-Uda [26],

Log-periodic [27] and surface wave antennas [28]. However, it is not easy to implement a low profile design without performance sacrifice. The SSPP offer a solution. In order to achieve the effective radiation of SSPP TL, periodic modulation and gradient truncation are the two most effective methods. Resonate elements can be used for periodic modulation or radiation director [13], [17]. I-shaped resonators and parasitic strips loaded in the endfire direction to increasing the directivity [18], [19]. But the bandwidth of these endfire antennas are narrow due to the dipole resonant nature. Based on the Vivaldi-shaped structure, a wide bandwidth can be obtained [20]. However, these SSPP antennas are designed on double-layer conductors, the single-layer conductors which is the significant advantage of SSPP TLs is not being exploited. Thus, it may simplify the fabrication and improve the radiation efficiency due to its groundless single-layer configuration. Previous works of SSPP endfire radiation is reported by tapering the fish-bone SSPP TLs [21]–[24]. Microstrip transition and CPW transitions are utilized to excite SSPP wave in [21] and [22]–[24] respectively.

In this paper, we propose a novel design of endfire antenna based on a SSPP groundless single-layer configuration. In comparison with previous work, this antenna need only a single metal layer makes it suitable for low-profile

The associate editor coordinating the review of this manuscript and approving it for publication was Shah Nawaz Burokur¹.

applications and easy fabrication. Meanwhile, we combine the asymmetric radiation elements of SSPP TL with a director to develop a high gain endfire antenna. It also leads to a wide operational frequency and a low profile, which is flush-mounted for aircraft, vehicle and wireless communications.

II. DESIGN OF ANTENNA

The geometry of the proposed SSPP endfire antenna is shown in Fig. 1. The overall size of the whole structure is $L \times W = 167 \text{ mm} \times 80 \text{ mm}$, which is fabricated on a Rogers RO4003C substrate with a dielectric constant of 3.38, substrate thickness of 1mm and loss tangent of 0.001. The thickness of metallic layer is 0.018 mm. The antenna can be divided into three parts including the transition, the radiator and the director, as shown in Fig. 1.

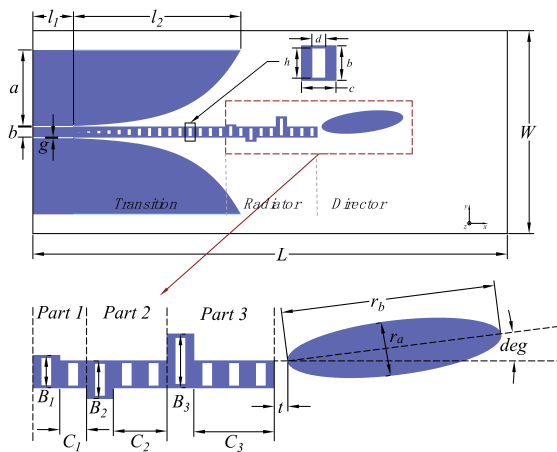


FIGURE 1. Configuration of the proposed SSPP endfire antenna.

In the transition part, the parameters of the CPW feeder are selected as $g = 0.5 \text{ mm}$, $l_1 = 16 \text{ mm}$, $l_2 = 66 \text{ mm}$, $a = 30 \text{ mm}$ and $b = 4 \text{ mm}$. The gradient slots and flaring grounds are designed to match the characteristic impedance of CPW to the SSPP TL and then reduce the reflection. Meanwhile, they convert the quasi-TEM mode to the SSPP mode smoothly. The SSPP transmission line is a corrugated metallic strip decorated with rectangular holes periodically. The dimensions of the unit cell are as follows: $c = 4 \text{ mm}$, $b = 4 \text{ mm}$, $d = 1.6 \text{ mm}$ and $h = 3.5 \text{ mm}$.

The radiation part of this proposed antenna is composed of three radiation elements shown in Fig. 1. They are arranged in array along the x-axis direction asymmetrically, with size $B_1 = 4.8 \text{ mm}$, $B_2 = 5.6 \text{ mm}$, $B_3 = 8.0 \text{ mm}$ and distance $C_1 = 4 \text{ mm}$, $C_2 = 12 \text{ mm}$, $C_3 = 24 \text{ mm}$.

An elliptical patch is introduced as a director, whose minor axis and major axis are $r_a = 8 \text{ mm}$, $r_b = 32 \text{ mm}$ respectively. Besides, the distance between the radiator and the elliptical patch director is $t = 2 \text{ mm}$. With a rotation of $\text{deg} = 3^\circ$ around, the director can suppress the first side-lobe level of this proposed antenna and adjust the direction of the beam slightly by rotating itself.

III. WORKING PRINCIPLE

The SSPP TL is a single-layer conductor transmission line supporting surface plasmon-like mode which is also a kind of surface wave. Its transmission characteristic is studied as shown in Fig. 2. The dispersion curves exhibit the SPP-like transmission behavior, and they present an asymptote to be mainly controlled by the height h of the rectangular TL holes as shown in Fig. 2. The dispersion curves of SSPP TL with different height h deviate gradually from the light line. The larger the height h is, the higher is its confinement and the lower is its cut-off frequency.

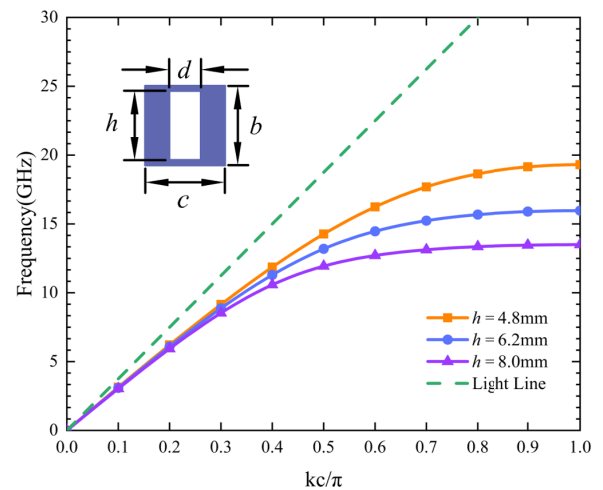


FIGURE 2. Dispersion curve of the unit cell in SSPP TL.

Since electromagnetic waves are tightly confined around SSPP TL, truncation and modulation of the TL are the easiest ways to generate the radiation. However, as shown in Fig. 3(a), the reflection coefficient is high and the total efficiency is low by this simple way. From the electric field distribution in Fig. 4(a), we can see that all the energy is reflected back and still tightly confined around the transmission line. In order to convert the SSPP mode wave to the space mode wave, a matching branch has been added. Then the improvement can be seen in the Fig. 3(b), the efficiency is greatly improved and return loss is reduced to -10 dB . However, its radiation pattern does not converge in one direction, as shown in Fig. 4(b).

To enhance the endfire radiation and expand the bandwidth, three gradient cells cascade as Part1, Part 2 and Part 3 in radiator as shown in Fig. 1. The periodic elements on both sides of the transmission line gradually get larger. The operating bandwidth is down to $15.75\text{--}17.5 \text{ GHz}$, and the total efficiency is up to 95% , as shown in Fig. 3(c). From electric field distribution in Fig. 4 (c), we can see the endfire radiation obviously. However, its radiation pattern is slightly split, as shown in Fig. 5. Thus, an elliptical patch is introduced as a director to guide the radiation and suppress the first side-lobe. Meanwhile, the beam angle of the radiation direction is adjusted. Finally, simulation results of the proposed

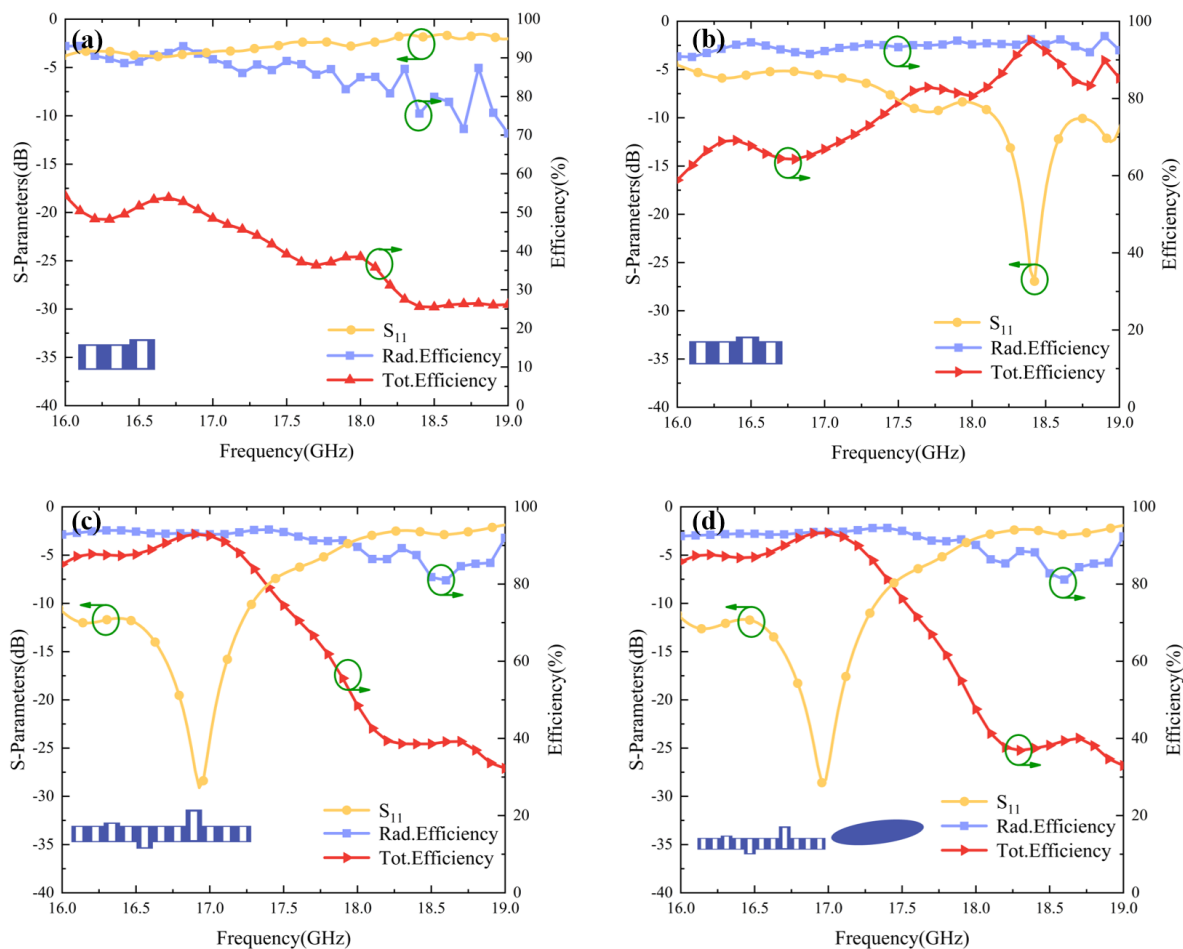


FIGURE 3. Reflection coefficient, radiation efficiency and total efficiency of different elements in Fig. 1. (a) Effects of part1. (b) Effects of part1 and matching branch. (c) Effects of part1,2,3 in antenna. (d) Effects of part1,2,3 and director in antenna.

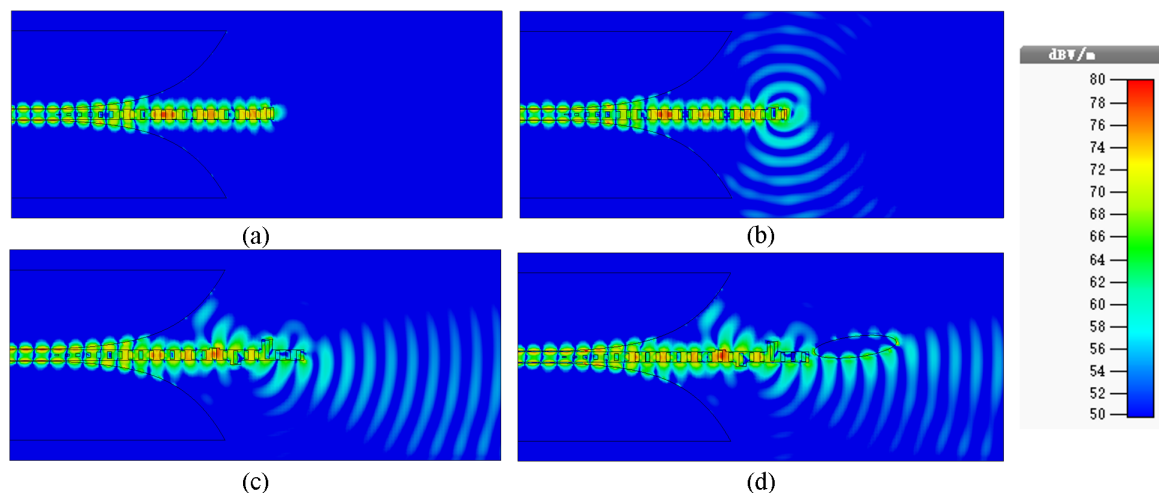


FIGURE 4. Electric field distribution of different structure. (a) truncation. (b) one cell of truncation and matching branch. (c) three cells of truncation and matching branch. (d) three cells and a director.

antenna are shown in Fig. 3(d) and Fig. 4(d). It can be seen that director does not affect the performance of reflection coefficient and efficiency, but improve the radiation pattern.

The radiation patterns comparison for the proposed antenna with and without director at 17 GHz are illustrated in Fig. 5 respectively.

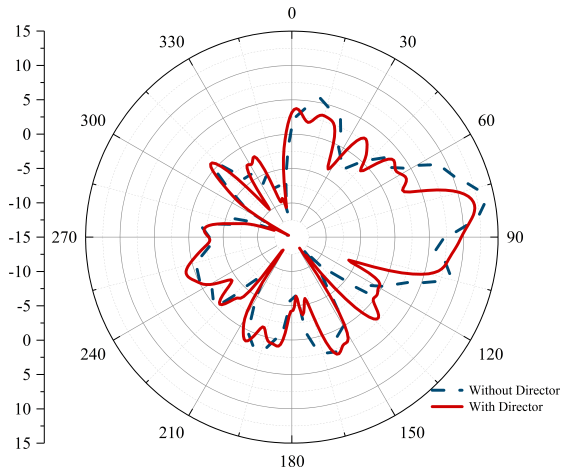


FIGURE 5. Comparison of the radiation pattern in the xy-plane.

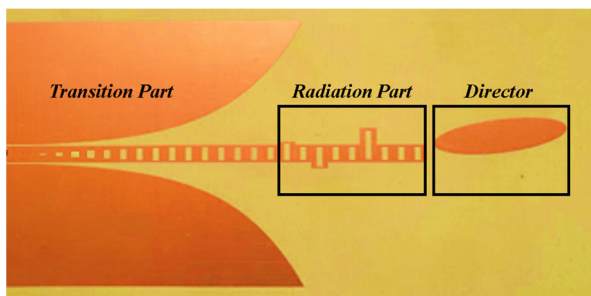


FIGURE 6. Prototype of the proposed antenna.

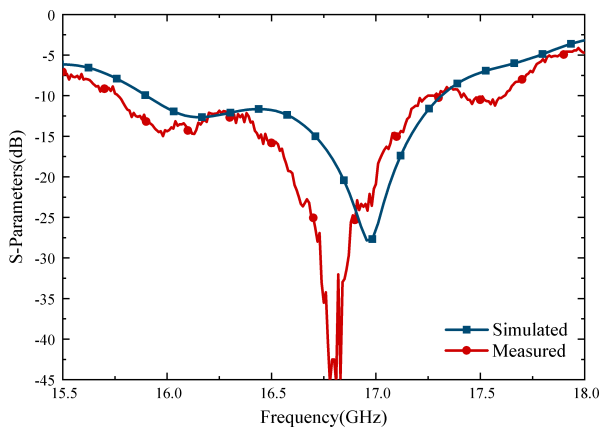


FIGURE 7. Measured and simulated scattering parameters of the SSPP antenna.

IV. FABRICATED ANTENNA AND MEASURED RESULTS

A prototype of the proposed antenna is fabricated for measurements in Fig. 6 and its geometrical parameters are shown in Fig. 1. Its simulated and measured scattering parameters are shown in Fig. 7. Both measured and simulated reflection coefficients are below -10 dB within the frequency range from 15.75 to 17.5 GHz, representing good impedance matching. There is a frequency deviation about 1.1%, which

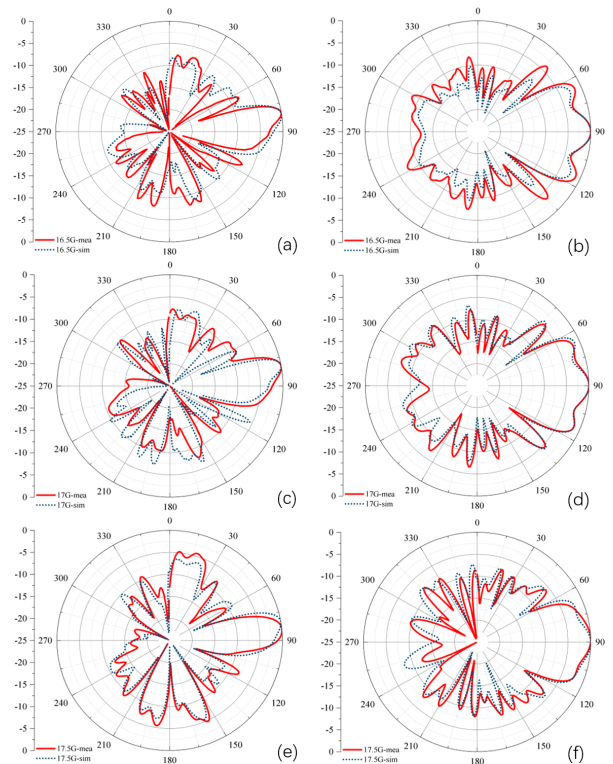


FIGURE 8. Measured and simulated radiation patterns of the proposed antenna. (a) (c) (e) xy-plane patterns at 16.5, 17 and 17.5 GHz, respectively. (b) (d) (f) xz-plane at 16.5, 17 and 17.5 GHz, respectively.

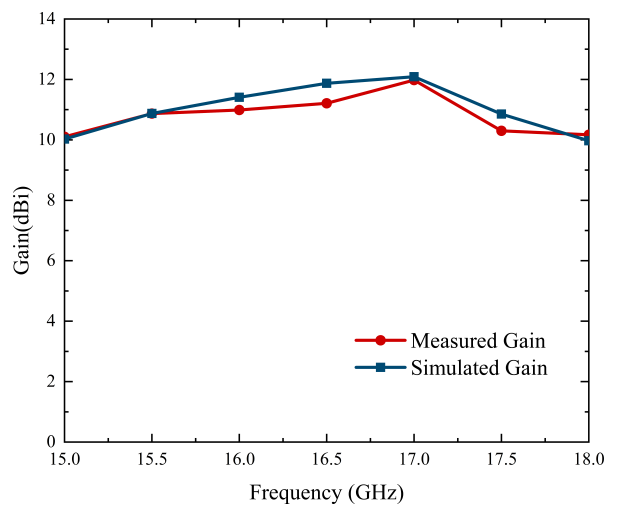


FIGURE 9. Measured and simulated gain of the SSPP antenna.

could be caused by fabrication errors and different relative permittivity of the substrate.

The simulated and measured normalized radiation patterns in the xy-plane and xz-plane at 16.5, 17 and 17.5 GHz are shown Fig. 8, respectively. The proposed SSPP antenna has been experimentally proven to operate endfire radiation. Simulated and measured gains of the proposed antenna are agreed well as shown in Fig. 9. The antenna achieves a high gain from 10.5 to 12.1 dBi overall the operation band.

TABLE 1. Performance comparison of SSPP endfire antennas.

Ref.	Type	Length (λ_0)	Gain (dBi)	f_0 (GHz)	BW
[25]	Leaky wave	6	-2-10.8	5	20%
[26]	Microstrip Yagi	1.7	7.2-8.9	5	8%
[27]	Log-periodic	2.34	6-10.9	30.5	62%
[28]	Surface wave	3.5	7.0-11.8	3.95	8.4%
[17]	Double SSPP	5	8.5 - 15.5	24.75	23%
[18]	Double SSPP	2.3	7.0 - 7.0	6.1	3%
[19]	Double SSPP	3.3	2.7 - 7.8	5.5	7%
[22]	Single SSPP	4.8	8.5 - 10.7	14.0	14%
[23]	Single SSPP	2.9	7.5 - 9.2	8.0	12%
[24]	Single SSPP	3.7	7.1 - 9.0	5.05	8%
Ours	Single SSPP	5.8	10.5 -12.1	16.6	11%

Table 1 compares the proposed antenna with other types of endfire antennas and other SSPP endfire antennas in the open literature. The frequency f_0 is the center frequency of bandwidth and λ_0 is wavelength in free space at f_0 . By saving large area of metal ground, the groundless single-layer configuration in SSPP antennas is more effective in integrated circuits and conformal applications. Moreover, since its electromagnetic waves tightly confined around the metal surface, the substrate loss and dielectric constant requirements of SSPP antennas are low. It is necessary to note that although the single-layer SSPP antenna requires a large geometrical size of transition, this transition is not need in an overall SSPP circuit system. Double-layer SSPP are easier to implement the endfire radiation with better performance than the single-layer ones since their electric dipole equivalent. As shown in Table 1, although the proposed antenna designed in a single-layer, it still achieve a high gain, even better than some double-layer works. By the comparisons, we can also see that different types of antennas have their own advantages and disadvantages. Leaky wave antenna and log-periodic antenna usually have a wide relative bandwidth, but the gain fluctuates and the side lobe level is high. Microstrip Yagi antenna is designed in compact dimensions by sacrificing the gain and bandwidth. Surface antennas are usually thick and a big conductor ground plane needed. SSPP antennas provide another way to implement a single-layer prototype with high gain endfire radiation.

V. CONCLUSION

In this paper, a low profile SSPP endfire antenna is proposed. To inherit the advantages of SSPP, the proposed antenna is designed based on a planar single-layer conductor on a Rogers RO4003C substrate. By implementing asymmetric modulation and truncation of the SSPP TL, the SSPP wave is converted to the space wave with an efficiency of 95%. The proposed antenna achieves a high gain from 10.5 to 12.1 dBi from 15.75 to 17.5 GHz. The antenna is then fabricated and measured to validate the working mechanism and predicted

radiation performance. The advantages of its single-layer, high gain and low profile demonstrate the proposed antenna a great potential in wireless communications.

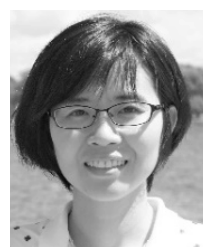
REFERENCES

- [1] W. L. Barnes, A. Dereux, and T. W. Ebbesen, "Surface plasmon subwavelength optics," *Nature*, vol. 424, no. 6950, pp. 824–830, Aug. 2003.
- [2] S. A. Maier, S. R. Andrews, L. Martín-Moreno, and F. J. García-Vidal, "Terahertz surface plasmon-polariton propagation and focusing on periodically corrugated metal wires," *Phys. Rev. Lett.*, vol. 97, no. 17, Oct. 2006, Art. no. 176805.
- [3] F. J. García-Vidal, L. Martín-Moreno, and J. B. Pendry, "Surfaces with holes in them: New plasmonic metamaterials," *J. Opt. A, Pure Appl. Opt.*, vol. 7, no. 2, pp. S97–S101, Feb. 2005.
- [4] C. R. Williams, S. R. Andrews, S. A. Maier, A. I. Fernández-Domínguez, L. Martín-Moreno, and F. J. García-Vidal, "Highly confined guiding of terahertz surface plasmon polaritons on structured metal surfaces," *Nature Photon.*, vol. 2, no. 3, pp. 175–179, Mar. 2008.
- [5] Q. Gan, Z. Fu, Y. J. Ding, and F. J. Bartoli, "Ultrawide-bandwidth slow-light system based on THz plasmonic graded metallic grating structures," *Phys. Rev. Lett.*, vol. 100, no. 25, Jun. 2008, Art. no. 256803.
- [6] A. Pors, M. G. Nielsen, R. L. Eriksen, and S. I. Bozhevolnyi, "Broadband focusing flat mirrors based on plasmonic gradient metasurfaces," *Nano Lett.*, vol. 13, no. 2, pp. 829–834, Feb. 2013.
- [7] A. Kianinejad, Z. N. Chen, and C.-W. Qiu, "Low-loss spoof surface plasmon slow-wave transmission lines with compact transition and high isolation," *IEEE Trans. Microw. Theory Techn.*, vol. 64, no. 10, pp. 3078–3086, Oct. 2016.
- [8] L. Liu, Z. Li, B. Xu, P. Ning, C. Chen, J. Xu, X. Chen, and C. Gu, "Dual-band trapping of spoof surface plasmon polaritons and negative group velocity realization through microstrip line with gradient holes," *Appl. Phys. Lett.*, vol. 107, no. 20, Nov. 2015, Art. no. 201602.
- [9] Y. Jin Zhou, X.-X. Yang, and T. Jun Cui, "A multidirectional frequency splitter with band-stop plasmonic filters," *J. Appl. Phys.*, vol. 115, no. 12, Mar. 2014, Art. no. 123105.
- [10] J. Y. Yin, J. Ren, H. C. Zhang, B. C. Pan, and T. J. Cui, "Broadband frequency-selective spoof surface plasmon polaritons on ultrathin metallic structure," *Sci. Rep.*, vol. 5, Feb. 2015, Art. no. 8165.
- [11] B. C. Pan, Z. Liao, J. Zhao, and T. J. Cui, "Controlling rejections of spoof surface plasmon polaritons using metamaterial particles," *Opt. Express*, vol. 22, no. 11, pp. 13940–13950, Jun. 2014.
- [12] H. C. Zhang, S. Liu, X. S. Hen, L. H. Chen, L. Li, and T. J. Cui, "Broadband amplification of spoof surface plasmon polaritons at microwave frequencies," *Laser Photon. Rev.*, vol. 9, no. 1, pp. 83–90, 2015.
- [13] L. Liu, M. Chen, J. Cai, X. Yin, and L. Zhu, "Single-beam leaky-wave antenna with lateral continuous scanning functionality based on spoof surface plasmon transmission line," *IEEE Access*, vol. 7, pp. 25225–25231, 2019.
- [14] Q. Zhang, Q. Zhang, and Y. Chen, "Spoof surface plasmon polariton leaky-wave antennas using periodically loaded patches above PEC and AMC ground planes," *IEEE Antennas Wireless Propag. Lett.*, vol. 16, pp. 3014–3017, 2017.
- [15] G. S. Kong, H. F. Ma, B. G. Cai, and T. J. Cui, "Continuous leaky-wave scanning using periodically modulated spoof plasmonic waveguide," *Sci. Rep.*, vol. 6, Jul. 2016, Art. no. 29600.
- [16] D. Liao, Y. Zhang, and H. Wang, "Wide-angle frequency-controlled beam scanning antenna fed by standing wave based on the cutoff characteristics of spoof surface plasmon polaritons," *IEEE Antennas Wireless Propag. Lett.*, vol. 17, no. 7, pp. 1238–1241, Jul. 2018.
- [17] X.-F. Zhang, W.-J. Sun, and J.-X. Chen, "Millimeter-wave ATS antenna with wideband-enhanced endfire gain based on coplanar plasmonic structures," *IEEE Antennas Wireless Propag. Lett.*, vol. 18, no. 5, pp. 826–830, May 2019.
- [18] J. Y. Yin, D. Bao, J. Ren, H. C. Zhang, B. C. Pan, Y. Fan, and T. J. Cui, "Endfire radiations of spoof surface plasmon polaritons," *IEEE Antennas Wireless Propag. Lett.*, vol. 16, pp. 597–600, 2017.
- [19] D. Tian, R. Xu, G. Peng, J. Li, Z. Xu, A. Zhang, and Y. Ren, "Low-profile high-efficiency bidirectional endfire antenna based on spoof surface plasmon polaritons," *IEEE Antennas Wireless Propag. Lett.*, vol. 17, no. 5, pp. 837–840, May 2018.

- [20] J. Y. Yin, H. C. Zhang, Y. Fan, and T. J. Cui, "Direct radiations of surface plasmon polariton waves by gradient groove depth and flaring metal structure," *IEEE Antennas Wireless Propag. Lett.*, vol. 15, pp. 865–868, 2016.
- [21] X. Du, H. Li, and Y. Yin, "Wideband fish-bone antenna utilizing odd-mode spoof surface plasmon polaritons for end-fire radiation," *IEEE Trans. Antennas Propag.*, vol. 67, no. 7, pp. 4848–4853, July 2019.
- [22] S. Ge, Q. Zhang, A. K. Rashid, G. Zhang, C.-Y. Chiu, and R. D. Murch, "Analysis of asymmetrically corrugated goubau-line antenna for endfire radiation," *IEEE Trans. Antennas Propag.*, vol. 67, no. 11, pp. 7133–7138, Nov. 2019.
- [23] A. Kandwal, Q. Zhang, X.-L. Tang, L. W. Liu, and G. Zhang, "Low-profile spoof surface plasmon polaritons traveling-wave antenna for near-endfire radiation," *IEEE Antennas Wireless Propag. Lett.*, vol. 17, no. 2, pp. 184–187, Feb. 2018.
- [24] K. Zhuang, J. Geng, K. Wang, H. Zhou, Y. Liang, X. Liang, W. Zhu, R. Jin, and W. Ma, "Pattern reconfigurable antenna applying spoof surface plasmon polaritons for wide angle beam steering," *IEEE Access*, vol. 7, pp. 15444–15451, 2019.
- [25] P. Liu, H. Feng, Y. Li, and Z. Zhang, "Low-profile EndFire leaky-wave antenna with air media," *IEEE Trans. Antennas Propag.*, vol. 66, no. 3, pp. 1086–1092, Mar. 2018.
- [26] J. Shi, L. Zhu, N.-W. Liu, and W. Wu, "A microstrip yagi antenna with an enlarged beam tilt angle via a slot-loaded patch reflector and pin-loaded patch directors," *IEEE Antennas Wireless Propag. Lett.*, vol. 18, no. 4, pp. 679–683, Apr. 2019.
- [27] G. Zhai, Y. Cheng, Q. Yin, S. Zhu, and J. Gao, "Gain enhancement of printed log-periodic dipole array antenna using director cell," *IEEE Trans. Antennas Propag.*, vol. 62, no. 11, pp. 5915–5919, Nov. 2014.
- [28] Y. Zhao, Z. Shen, and W. Wu, "Wideband and low-profile H-Plane ridged SIW horn antenna mounted on a large conducting plane," *IEEE Trans. Antennas Propag.*, vol. 62, no. 11, pp. 5895–5900, Nov. 2014.



MINGHONG CHEN was born in Jingjiang, Jiangsu, China, in 1994. He received the B.S. degree in electrical engineering from the Nanjing University of Posts and Telecommunications, Nanjing, China, in 2017, where he is currently pursuing the M.S. degree in electromagnetic field and microwave technology. His current research interests include metamaterials and leaky-wave antenna.



LEILEI LIU (Member, IEEE) received the B.Sc. and Ph.D. degrees in electromagnetic and microwave technology from Southeast University, Nanjing, China, in 2003 and 2009, respectively. She studied in Linnaeus University, Kalmar, Sweden, as an International Student, in 2004. Since 2009, she has been a Professor with the Nanjing University of Posts and Telecommunications, Nanjing. From 2015 to 2016, she was a Visiting Scholar with the Poly-Grames Research Center, Montreal, QC, Canada. Her current research interests include antennas, microwave components, and metamaterials.



XIAOXING YIN (Member, IEEE) was born in Taiyuan, China. He received the B.Sc. degree in radio engineering and the M.Sc. and Ph.D. degrees in electrical engineering from the Nanjing Institute of Technology (now Southeast University), Nanjing, China, in 1983, 1989, and 2001, respectively.

From 1983 to 1986, and 1989 to 1998, he was with the Department of Physics, University of Petroleum, Dongying, China, where he conducted research in the areas of logging methods and instruments. Since 2001, he has been with the State key Laboratory of Millimeter Waves, Southeast University, first as a Lecturer, now as a Professor. He has published 63 technical articles and holds over 30 patents. His current research interests include computational electromagnetics, microwave components and systems, and antennas.

...